HHS Public Access

Author manuscript

Dent Mater. Author manuscript; available in PMC 2017 October 01.

Published in final edited form as:

Dent Mater. 2016 October ; 32(10): 1270–1280. doi:10.1016/j.dental.2016.07.009.

COMPOSITION OF ELASTIN LIKE POLYPEPTIDE-COLLAGEN COMPOSITE SCAFFOLD INFLUENCES *IN VITRO* OSTEOGENIC ACTIVITY OF HUMAN ADIPOSE DERIVED STEM CELLS

Bhuvaneswari Gurumurthy[1], **Patrick C. Bierdeman**[1], and **Amol V. Janorkar**[*]

Department of Biomedical Materials Science, School of Dentistry, University of Mississippi Medical Center, Jackson, Mississippi, 39216

Abstract

Objectives—Collagen-based scaffolds for guided bone regeneration (GBR) are continuously improved to overcome the mechanical weaknesses of collagen. We have previously demonstrated superior mechanical characteristics of the elastin-like polypeptide (ELP) reinforced collagen composites. The objectives of this research were to evaluate the efficacy of ELP-collagen composites to culture human adipose-derived stem cells (hASCs) and allow them to undergo osteogenic differentiation. We hypothesized that hASCs would show a superior osteogenic differentiation in stiffer ELP-collagen composites compared to the neat collagen hydrogels.

Methods—Composite specimens were made by varying ELP (0–18 mg/mL) and collagen (2–6 mg/mL) in a 3:1 ratio. Tensile strength, elastic modulus, and toughness were determined by uniaxial tensile testing. hASCs cultured within the composites were characterized by biochemical assays to measure cell viability, protein content, and osteogenic differentiation (alkaline phosphatase activity, osteocalcin, and Alizarin red staining). Scanning electron microscopy and energy dispersive spectroscopy was used for morphological characterization of composites.

Results—All composites were suitable for hASCs culture with viable cells over the 22-day culture period. The ELP-collagen composite with 18 mg/mL of ELP and 6 mg/mL of collagen had greater tensile strength and elastic modulus combined with higher osteogenic activity in terms of differentiation and subsequent mineralization over a period of 3 weeks compared to other compositions. The extra-cellular matrix deposits composed of calcium and phosphorous were specifically seen in the 18:6 mg/mL ELP-collagen composite.

Significance—The success of the 18:6 mg/mL ELP-collagen composite to achieve long-term, 3-dimensional culture and osteogenic differentiation of indicates its potential as a GBR scaffold.

[*]Corresponding author: Telephone: (601) 984-6170; Fax: (601) 984-6087; ajanorkar@umc.edu.

[1]Equal contribution

Keywords

Elastin-like polypeptide; Collagen; Bone tissue engineering; Human adipose derived stem cells; Osteogenic differentiation; Composite scaffold; Guided bone regeneration; Elastic modulus

1. INTRODUCTION

Periodontitis is the inflammation of the periodontium surrounding the tooth with progressive loss of alveolar bone resulting in complete loosening of the tooth. Guided bone regeneration (GBR) and guided tissue regeneration (GTR) are widely used techniques that regenerate the various periodontal tissues including the root cementum, periodontal ligaments, and alveolar bone, thereby decreasing the mobility of the affected tooth [1–3]. GTR uses a resorbable or non-resorbable membrane as a barrier between the epithelial and connective tissues. This membrane prevents the unwanted re-growth of the epithelial and connective tissues [3]. GBR uses a resorbable or non-resorbable scaffold to support the regeneration of the alveolar bone at a bony defect introduced by tooth extraction or disease [3]. The materials used in GBR/GTR must be biocompatible, non-immunogenic, and non-inflammatory. In addition, the GBR/GTR materials must possess adequate strength to allow proper handling for their placement at the defect site and modulus to avoid collapse under the intraoral forces. Finally, the GBR/GTR materials must degrade *in vivo* at a rate that matches the rate of the new tissue formation [3].

The current trend in periodontal tissue engineering research is focused toward bone regeneration at targeted sites by combining stem cells, scaffolds, and growth factors. Human mesenchymal stem cells (MSCs) are an attractive source of stems cells for bone regeneration as they have the capacity to regenerate and differentiate into osteogenic lineage [4]. Human adipose-derived stem cells (hASCs) have emerged as an alternative to human bone marrow MSCs (hBMSCs) due to their easy procurement from liposuction patients, rapid *in vitro* expansion, and high harvest yield [5]. hASCs have a demonstrated ability to differentiate into osteoblastic lineage *in vitro* as well as in the clinical treatment of bone defects [6–8]. Therefore, for this research, we have used hASCs to evaluate their osteogenic function in different scaffolds. For GBR applications, scaffolds act as the housing in which the osteoregenerative cells like hASCs can proliferate, differentiate, and mineralize into bone. Successful biocompatible scaffolds should possess adequate mechanical and resorption properties [3] along with suitable osteoconductive and osteoinductive properties. Unfortunately, the currently available synthetic scaffolds prove inadequate for clinical applications. For instance, the non-resorbable scaffolds require a second surgery for their removal, causing economic and physical discomfort for the patient [3]. Synthetic resorbable polymers suffer from early loss of structural and mechanical properties with poor cell response [9, 10]. Natural resorbable polymers such as collagen are osteoinductive and an effective alternative to synthetic polymers due to their biocompatibility and excellent cell affinity [11–13]. However, they often suffer from rapid hydrolytic and enzymatic degradation and lack sufficient mechanical properties [14, 15]. Crosslinking of collagen using chemicals [3] like glutaraldehyde and 1-ethyl-3-(3-dimethylaminopropyl) carbodiimide hydrochloride can overcome poor mechanical properties and antigenicity but

the possibility of cytotoxicity increases [16, 17]. Blending of collagen with other polymers and ceramics have shown to enhance mechanical properties and modulate specific cellular responses [18–21]. These disadvantages of both non-resorbable and resorbable materials make it clear that an “ideal” material has not been found [22] and have led to approaches that use non-crosslinked collagen composites [3].

In the design of bio-inspired bone regenerative composites with non-crosslinked collagen, elastin-like polypeptides (ELP) are under investigation as they have amino acid sequences similar to native elastin [23]. ELP, which is a soluble and recombinant form of elastin, offers an attractive solution to the problems faced by non-resorbable and resorbable synthetic materials used previously to prepare collagen-based composites. ELPs display inverse phase transition behavior which allows easy purification [20]. More importantly, ELPs possess excellent mechanical properties [24]. In the past, we prepared non-crosslinked ELP-collagen composites by utilizing the gelation behavior of collagen at 37°C and showed their superior mechanical behavior and equivalent biocompatibility compared to neat collagen hydrogels [24, 25]. We demonstrated that ELP-collagen composite scaffolds help in the attachment, proliferation, and subsequent differentiation of 3T3-E1 mouse pre-osteoblastic cells [25].

Mechanical properties such as stiffness or modulus play a crucial role in the success of a scaffold and also influence the commitment of cells to a specific lineage. Studies have shown that osteogenic differentiation is stiffness/ modulus dependent in hBMSCs [26, 27]. Huebsch *et al.* showed that both human and murine MSCs cultured in the presence of mixed osteogenic and adipogenic supplements can be made to undergo either adipogenic or osteogenic differentiation based on the matrix stiffness [28]. Though the effect of matrix stiffness has been well studied with hBMSCs, the lacuna with hASCs led to the development of this study. We aimed to study the effect of scaffold composition and stiffness on the ability of hASCs to commit to osteogenic lineage. We hypothesized that hASCs would differentiate along the osteoblastic lineage in a more rigid ELP-collagen composite compared to the neat collagen hydrogels. Hence, we investigated the efficacy of composites made with varying concentrations of ELP and collagen for hASCs culture to produce viable and differentiated osteoblast-like cells and investigated the influence of mechanical properties like elastic modulus of the composites on the osteogenic differentiation.

2. MATERIALS AND METHODS

2.1 Expression and Purification of ELP

Preparation of ELP was performed as described elsewhere [25]. Briefly, *Escherichia coli* BLR(DE3) bacteria (Novagen, Madison, WI, USA) with synthetic gene for ELP having primary sequence of [Valine-Proline-Glycine-Valine-Glycine]$_{120}$ were cultured for 24 h at 37°C and lysed by sonication. The inverse phase transition behavior of ELP was used for purification by three repeated cycles of solubilization in deionized water at 4°C, followed by precipitation and centrifugation at 40°C. The ELP solution was dialyzed and then lyophilized (Labconco Corp, Kansas City, MO, USA).

2.2 Preparation of Composites for Mechanical Testing

Collagen type I (9 mg/mL, rat tail, Invitrogen, Carlsbad, CA, USA) and ELP were mixed at varying concentrations to form four different compositions, namely, H1: 0 mg/mL ELP + 2 mg/mL collagen, H2: 6 mg/mL ELP + 2 mg/mL collagen, H3: 0 mg/mL ELP + 6 mg/mL collagen, and H4: 18 mg/mL ELP + 6 mg/mL collagen (Table 1). To prepare H2 and H4 composites, ELP (6 mg/mL or 18 mg/mL) was first dissolved in sterile DI water and gently mixed with collagen (2 mg/mL or 6 mg/mL, respectively). Next, 1N NaOH and 10X PBS were added. To prepare the control H1 and H3 collagen hydrogels with no ELP, collagen (2 mg/mL or 6 mg/mL) was gently mixed with 1N NaOH and 10X PBS. 350 μL of the final solutions for H1, H2, H3, and H4 were incubated at 37°C and >70% humidity for 18 h per dog-bone shaped well of a custom-made acrylic mold for mechanical testing.

2.3 Mechanical Testing

The dog-bone shaped specimens ($n \geq 6$) were kept wet by immersion in PBS at 37°C and >70% humidity until they were tested on day 8. The dimensions of the specimens were measured using VHX Digital Microscope (Keyence Corp, Osaka, Japan) and Vernier calipers. Average thicknesses of the H2 and H4 ELP-collagen composites were 0.84 ± 0.30 and 1.47 ± 0.45 mm, respectively and were not statistically different ($p > 0.05$) from their respective H1 and H3 control collagen hydrogels (0.76 ± 0.33 and 1.54 ± 0.45, respectively). Average widths of the H1, H2, H3, and H4 composites were 3.25 ± 0.53, 2.89 ± 0.61, 3.32 ± 0.35, and 3.49 ± 0.34 mm, respectively. As expected, the widths of all composites were not statistically different ($p > 0.05$) since they were prepared in the custom-made, dog-bone shaped acrylic mold having precise width. Uniaxial testing was performed with ASTM D882 on a Sintech 2/G Materials Testing System (MTS, Eden Prairie, MN, USA) at an extension rate of 0.5 in/min (12.7 mm/min). Tensile strength, elastic modulus , and toughness were calculated using MTS Testworks 4.0 software.

2.4 Cell Culture

hASCs were obtained from an unidentified adult female patient who underwent liposuction in accordance with the protocol approved by the University of Mississippi Medical Center Institutional Review Board (IRB Approval # 2012–0004). hASCs were maintained and expanded at 37°C and 5% CO_2 in 50:50 Dulbecco's modified Eagle's medium (DMEM, HyClone Labs, South Logan, UT, USA) and F12 (Invitrogen, Carlsbad, CA, USA) supplemented with 10% calf serum, 1% penicillin-streptomycin, and 1 mM sodium pyruvate (Invitrogen, Carlsbad, CA, USA) with pH adjusted to 7.4. Cells were harvested using trypsin-EDTA at 80% confluence. These cells were seeded within the collagen and collagen-ELP composites as described below.

2.5 Preparation of Composites for Cell Culture

Four compositions (H1, H2, H3, and H4) were prepared as described above, except 10X DMEM containing 50,000 cells was used instead of 10X PBS. 200μL of the final solution was incubated per well of a 96-well tissue culture polystyrene plate (Costar, Corning Life Sciences, Lowell, MA, USA) at 37°C and >70% humidity for 18 h. All composites were prepared in triplicate. After 24-hour acclimation, the composites were supplemented with an

osteogenic cocktail containing DMEM, 50 microM L-ascorbic acid, 10 nM dexamethasone, 10 mM β-glycerophosphate, 10% fetal bovine serum, and 1% penicillin/streptomycin for 3 weeks. Fresh media was fed every 48 h.

2.6 Biochemical Analysis

All the assays were performed according to the manufacturers' protocols. Cell viability within the various composites was assessed on day 22 using a Live/Dead assay (Invitrogen, Carlsbad, CA, USA). The cells were washed with sterile PBS and Live/Dead reagents (4 μM EthD-1 and 2 μM calcein AM) were added. The composites were incubated for 25 min at 37°C. Observations were made by epifluorescence microscopy using an Olympus IX 81 microscope (Olympus America, Center Valley, PA, USA) equipped with a Slidebook image analysis software. The percentages of live and dead cells were calculated by measuring the fluorescence at 645 and 530 nm, respectively using a FLX-800 fluorescence plate reader (Biotek, Winooski, VT, USA).

For quantification of total protein content, alkaline phosphatase activity, and osteocalcin production, triplicates of H1, H2, H3, and H4 composites were removed from the plates to isolate the cells. The cells were first separated from the composites by digestion using 1 U/mL Liberase (Roche Diagnostics, Indianapolis, IN, USA) in $CaCl_2$ – Krebs Ringer buffer for 25 min at 37°C. The cells were then pelleted from the media via centrifugation at 3500 rpm for 5 min, washed with PBS, and spun again at 3500 rpm for 5 min. The cells were then resuspended in 300 μL of PBS, lysed by sonication at 10% amplitude for 30 s, and immediately frozen.

Total protein amount present in the samples of days 1, 8, 15, and 22 were measured using a BCA total protein assay kit (Thermo Scientific, Rockford, IL, USA). 50 parts of reagent A and 1 part of reagent B supplied by the manufacturer were mixed to form the working solution. 25 μL of the lysate was added to 200 μL of the working reagent, mixed on a shaker for 30 s, and incubated at 37°C for 20 min. The absorbance was measured at 540 nm on ELX-800 absorbance plate reader (Biotek, Winooski, VT).

A colorimetric kinetic determination of alkaline phosphatase (ALP) activity was performed using QuantiChrom ALP assay kit (BioAssay Systems, Hayward, CA, USA) on days 8, 15, and 22. In brief, 25 μL of the cell lysate was transferred into a 96-well plate along with 150 μL of working solution (10% v/v Magnesium acetate and 4% v/v p-nitrophenyl phosphate liquid substrate in assay buffer) and the absorbance was measured at 405 nm at 0 and 4 min on ELX-800 absorbance plate reader. The ALP activity was then calculated as per manufacturer's instructions.

A sandwich ELISA assay specific for human osteocalcin (OCN) was performed using osteocalcin assay kit (Invitrogen) on days 8, 15, and 22. In short, monoclonal antibodies bound to the human OCN in standards or samples (25 μL), were bound to a monoclonal antibody labeled with horse radish peroxidase (100 μL) for 2 h at room temperature. The surfaces were washed extensively with a wash solution and reacted to a chromogenic solution in the dark at room temperature for 30 min. The reaction was completed with 100

μL of the stop solution and absorbance was measured at 450 nm using ELX-80 absorbance plate reader. The OCN activity was then calculated as specified by the manufacturer.

Next, the osteogenesis quantitation kit (EMD Millipore, Billerica, MA, USA) was used to analyze mineralization on day 22. The cell-seeded composites were washed with PBS and fixed using 10% formaldehyde for 15 min. After further washing, the composites were incubated at room temperature for 20 min in 1 mL Alizarin red stain per well. The excess dye was removed by extensive washing with DI water. Mineral deposits in composites were stained bright red and visualized using VHX Digital Microscope. Quantitative analysis was performed by further incubating the composites in 10% acetic acid for 30 min with shaking, then vigorous vortexing for 30 s, and heating at 85 °C for 10 min. The extracted mixture was centrifuged at 22,000×g for 15 min and neutralized with 150 μL of 10% ammonium hydroxide. The absorbance of the solution was measured at 405 nm using ELX-800 absorbance plate reader.

2.7 Scanning electron microscopy (SEM) with energy dispersive spectroscopy (EDS)

The cell seeded composites were washed with sterile PBS and fixed in 4% paraformaldehyde for 1 h at room temperature. They were then dehydrated using ascending ethanol series of 50%, 70%, 80%, 90% and 100% ethanol for 10 min each. The composites were then dried in the desiccator overnight. The dried composites were mounted on aluminum SEM stubs using carbon adhesive tape and sputter-coated with gold for 2 min at 9V. The composites were observed with SUPRA 40 scanning electron microscope (Carl Zeiss, Thornwood, NY, USA) at 5 kV using both the in-lens detector and the Everhart-Thornley secondary electron detector. Images were recorded at least from two different areas on each composite at 5,000X and 10,000X magnifications. Energy dispersive spectroscopy was performed on H3 and H4 composites to determine the presence of phosphorus and calcium.

2.8 Statistical Analysis

Results have been reported as mean ± 95% confidence intervals. Results were analyzed using ANOVA and Games-Howell post hoc test for unequal variances in SPSS version 23 statistical software. Values with $p \leq 0.05$ were deemed significantly different.

3. RESULTS

3.1 Mechanical Testing

Table 2 shows the average values of tensile strength, elastic modulus, and toughness for the hydrated collagen hydrogels and ELP-collagen composites. The elastic modulus shows an increasing trend with the concentration of collagen and the addition of ELP. For instance, the average elastic modulus for the H3 hydrogel prepared using 6 mg/mL collagen was higher than that for the H1 hydrogel prepared using 2 mg/mL collagen. Similarly, the elastic modulus for the H4 ELP-collagen composite was higher than that for the H3 collagen hydrogel ($p = 0.087$). Interestingly, the elastic modulus values nearly doubled for the H4 composite (61.8 ± 22.7 kPa) compared to the other three composites ($p \leq 0.05$). Similar increasing trends were seen in tensile strength and toughness values.

3.2 Live/Dead Assay

The Live/Dead assay was performed to assess cell viability in the various composites at the end of the 3-week culture period. Figure 1 shows Live/Dead assay of hASCs cultured within the collagen hydrogels and ELP-collagen composites. For all the compositions, the live cells were in high numbers compared to the dead cells. The percentage of live and dead cells as calculated by measuring the corresponding green and red fluorescence showed that more than 90% of the cells were alive on day 22 in all the four groups of composites. These results corroborate our previous studies that showed the collagen and ELP-collagen composites supported excellent cell viability over a 3-week culture period [25,29].

3.3 Total Protein Assay

The total protein content of all cells cultured within the collagen hydrogels and ELP-collagen composites were measured on days 1, 8, 15, and 22. As shown in Figure 2, the total protein content of the hASCs cultured within the composites increased 2- to 4- folds from day 1 to day 8 for all the composites, after which the protein level plateaued. The total protein content of cells cultured on H1, H2, and H3 appeared similar ($p > 0.05$ against H1 on the same day). However, the total protein content of cells cultured in H4 was significantly lower on days 15 and 22 ($p \leq 0.001$ against H1 on the same day). For instance, the total protein content measured on day 22 for H1, H2, and H3 were 196.8 ± 25.2, 173.8 ± 15.7, and 149.8 ± 13.8 μg respectively, while the total protein content measured on day 22 for H4 was 52.7 ± 8.9 μg.

3.4 Normalized Alkaline Phosphatase (ALP) activity

The ALP activity normalized to the total protein content for hASCs cultured within the composites H1, H2, and H3 were similar on all the days in the range of ~10–30 nM/min/μg protein as seen in Figure 3 ($p > 0.05$ against H1 on the same day). However, the H4 composite showed significantly higher ALP activity of 44.0 ± 7.1 nM/min/μg protein on day 22 ($p = 0.001$ against H1 on the same day).

3.5 Normalized Osteocalcin (OCN) Production

The OCN production normalized to the total protein content by the hASCs cultured within the composites is shown in Figure 4. The OCN levels expressed by the cells were similar (~0.5 pg/μg protein) on all days for H1, H2, and H3 ($p > 0.05$ against H1 on same day). However, the H4 composite showed maximum OCN production of 1.6 ± 0.9 pg/μg protein ($p > 0.05$ against H1 on the same day) and 1.5 ± 0.0 pg/μg protein ($p < 0.05$ against H1 on the same day) on days 15 and 22, respectively.

3.6 Alizarin Red Staining

Figure 5 shows the micrographs of Alizarin red stained hASCs cultured within the composites for the 22-day culture period. Alizarin red staining showed no mineralization in H1 and H2 (Figures 5a and 5b) and very little mineralization in H3 (Figure 5c). In contrast, the cells cultured in H4 showed bright red staining throughout the composite indicating extensive mineralization (Figure 5d). The extent of mineralization was quantified by measuring the concentration of extracted Alizarin red stain (Figure 5e). The normalized

Alizarin red staining in H3 was 0.04 ± 0.01 pmol/μg protein ($p \leq 0.01$ against H1 on same day), while the H4 composite had significantly greater Alizarin red staining (1.62 ± 0.48 nmol/μg protein) ($p \leq 0.01$ against H1 on the same day).

3.7 Scanning electron microscopy with energy dispersive spectroscopy

Osteoblast like cells were seen in all the composites with the appearance of extracellular matrix deposits (Figure 6a–d). These deposits were more in number and formed flat, dense, large mineralized regions in H4 composite (Figures 6d) when compared to the deposits in H3 composite that were round, isolated, and scattered (Figures 6c). SEM paired with EDS to identify the elemental compositions of these deposits revealed only phosphorous-containing deposits indicating unmineralized matrix in the H3 composite while the H4 composite showed a high amount of calcium and phosphorous containing deposits indicating a mineralized matrix (Figure 7).

4. DISCUSSION

Collagen is abundantly present in the extra-cellular matrix of most tissues and is an important component of bone tissue. Although osteogenic differentiation is influenced by the interactions of cells with their extracellular matrix, the collagen based scaffolds have been shown to encourage cell differentiation in response to osteogenic differentiation media [30]. Commonly used in the clinical setting today, the collagen-only GBR scaffolds show excellent cell and tissue compatibility. Unfortunately, the collagen-only scaffolds suffer from uncontrolled degradation by naturally occurring collagenases, leading to their premature degradation and resulting in inadequate mechanical properties necessary for a successful GBR application [3]. Many studies have shown improved mechanical properties [31–33] and/or better bone formation [34] *in vitro* using collagen composite scaffolds. Here, by incorporating ELP and hASCs we aimed to improve the collagen scaffolds in terms of their mechanical and biochemical properties for their effective use in bone tissue engineering.

We chose ELP to improve the mechanical properties of the composites because ELP is similar to mammalian elastin that provides strength and extensibility to the extracellular matrix. We have previously shown that the addition of ELP improved the mechanical properties like tensile strength and elastic modulus of ELP-collagen composites as well as enhanced osteoblastic differentiation of the 3T3-E1 mouse pre-osteoblasts [25]. In this study, we used a 3:1 w/w ELP to collagen ratio, thereby reducing the collagen content to only 25% w/w. In our composites, ELP thus became the major component as the filler reinforcing the collagen matrix and increased the rigidity of the composite. We have previously shown the presence of extensive molecular entanglements and inter and intra-molecular secondary bonding interactions between ELP and collagen [24]. Such interactions lead to reinforcement of the collagen matrix by ELP and increase the tensile strength and elastic modulus of the composites as seen in Table 1. The H4 composite had a two-fold increase in modulus when compared to H1, showing that with increase in concentration and density of the matrix, modulus has increased. Our results followed a similar trend as the study conducted by Brougham et al. where the incorporation of fibrin into a collagen-glycosaminoglycan scaffold had increased the modulus of the scaffold significantly when

compared to a fibrin-only scaffold [33]. The H4 composite developed in this study has a tensile strength of 20.2 ± 11.3 kPa and modulus of 61.8 ± 22.7 kPa. Our values are similar to the study conducted by Engler et al. where an elastic modulus of 25–40 kPa was considered to be osteogenic with inert polyacrylamide gels in which the concentration of bis-acrylamide crosslinking sets the elasticity and the cellular adhesion was provided by coating the gels with collagen type I [35]. However, these values are significantly lower than those for the vacuum-dried poly(ethylene glycol dimethacrylate) hydrogels (tensile strength = 6.2 MPa and modulus = 2.0 MPa) as reported by Killion et al. [36] and the microporous bacterial cellulose scaffold (tensile strength = 0.27 MPa and elastic modulus = 1.6 MPa) as reported by Zabarowska et al. [37]. This indicates scope for further improvement in the mechanical characteristics of our composites without negatively impacting the osteogenic activity.

We used hASCs to improve the biochemical properties of the scaffolds because of their high proliferation rate and osteogenic differentiation capacity in cell culture [6]. This ability has also been demonstrated when hASCs were encapsulated in fibrin/hyaluronic acid hydrogel-coated polycaprolactone/poly(lactic-co-glycolic acid) scaffold, electrospun poly(L-lactic acid)/tricalcium phosphate scaffold, and electrospun biphasic calcium phosphate/polycaprolactone-nano hydroxyapatite scaffold [38–40]. To this end, we evaluated the ability of the ELP-collagen composites to support bone formation by hASCs. To identify the effect of composition of ELP and collagen on osteogenic activity of hASCs, we used four different composites with varying collagen and ELP compositions. Neat collagen hydrogels had 2 mg/mL and 6 mg/mL of collagen. The amount of ELP used was three times the concentration of collagen, making it 6 mg/mL and 18 mg/mL in the ELP-collagen composites. In our study, the hASCs cultured within all the four scaffold formulations displayed an initial increase in the total protein content from day 1 to day 8 indicating increased cell proliferation activity in all composites (Figure 2). By day 15, the hASCs began to show reduced proliferation activity indicated by the plateaued protein levels. Such behavior of an initial increase followed by a plateau in total protein content is in accordance with the reciprocal relationship between proliferation and differentiation along the osteogenic lineage, wherein a decreasing proliferation gives way to differentiation [41], followed by maturation. This behavior was more appreciable in the H4 composite that utilized the higher concentration of ELP and collagen (18:6 mg/mL). Thus the possible continual, albeit slower, proliferation in the H1, H2, and H3 composites may have contributed to the lower differentiation and mineralization pattern seen in the ALP activity, OCN production, and Alizarin red staining (Figures 3, 4, and 5). In view of varying cellular content in all our composites, the normalization of ALP activity, OCN production, and Alizarin red staining with total protein content was done to show that the increased differentiation, maturation, and mineralization were not an effect of increased number of hASCs in a particular composite. The hASCs cultured within all the four scaffold formulations displayed equivalent viability on day 22, confirming the well-known biocompatibility of collagen and ELP over a long-term cell culture period (Figure 1).

Alkaline phosphatase, found on the surface of osteoblasts is believed to be a marker of early osteoblastic differentiation as its level increases with maturation of osteoblasts [42–44]. ALP activity correlates with bone matrix formation prior to the initiation of mineralization [45]. The initial spike in normalized ALP activity on day 15 (Figure 3), indicated that the hASCs

started to undergo initial differentiation, in which they started forming the extracellular matrix. Interestingly, the normalized ALP activity in the H4 composite was higher than all the other composites (Figure 3). These results matched with an earlier report by Tan et al. that showed increased osteogenic differentiation characterized by ALP activity and Alizarin red staining primarily occurred in a stiff microenvironment with 6% and 9% transglutaminase-crosslinked gelatin (TG) gels when compared to a soft matrix of 3% TG gel [26]. This is also in line with a study performed by Gandavarapu et al., who used thiolene chemistry to functionalize poly(ethylene glycol) hydrogels with a pendant peptide moiety and found that stiffer gels with Young's modulus of 25 kPa had increased ALP activity on day 14 than the softer hydrogels with a modulus of 2 kPa [46]. Furthermore, OCN is the most abundant non-collagenous protein in bone extracellular matrix [47] and its expression is closely related to bone metabolism including bone extracellular matrix mineralization and turnover [48]. Figure 4 demonstrates the results of OCN assay on different composites. The cells in H4 composite produced more OCN over the 22 day period than all the other composites. Continuing after osteogenic differentiation, hASCs begin to secrete a matrix which further mineralizes to form bone. The qualitative and quantitative assessment of mineralized deposits by Alizarin red staining (Figure 5) showed that, the cells that were encapsulated by the H4 composite formed a mineralized matrix to a significantly greater extent than all the other composites. The stain color of the deposits became as darker/thicker red from H1 to H4 composites with the increase in collagen concentration from 2 to 6 mg/mL, similar to the observation of Thein-Han and Xu in collagen-calcium phosphate cement scaffold with increasing collagen fibers concentration from 0 to 8% [49].

The presence of collagen in our composites provides a favorable environment for the cell attachment and proliferation. Since collagen is a natural ECM protein, the cells readily attach to collagen with the help of cell surface receptors including $\alpha_1\beta_1$ and $\alpha_2\beta\alpha_1\beta_1$ and $\alpha_2\beta_1$ integrins [50–52], and show increased proliferation due to cell to cell and cell to matrix interactions in a 3D in vivo like environment [53]. Additionally, in our composites, the presence of ELP enhances the stiffness of the composite and thereby favors differentiation and mineralization [26]. The highest mineralization in the high concentration ELP-collagen H4 composite is in line with greater ALP activity and OCN production. These results were further corroborated by the SEM and EDS data (Figure 7). EDS revealed the presence of high amount of calcium and phosphorous deposits indicating extensive mineralization in the H4 composite compared to the control collagen-only H3 hydrogel. Correlating the SEM, EDS and biochemical data, we can infer that the collagen-only H1 and H3 hydrogels and the ELP-collagen H2 composite that utilized the lower concentration of ELP and collagen (6:2 mg/mL) had a slower differentiation and maturation rate in the given 22 day culture period and the cells in these composites had only matured to form an unmineralized matrix.

Taken together, the normalized ALP activity, OCN production, and mineralization were higher in the H4 composite compared to all the other composites (Figures 3, 4, and 5). Thus the H4 composite that utilized the higher concentration of ELP and collagen (18:6 mg/mL) performed better mechanically, biochemically, and morphologically and displayed a closer resemblance to the natural bone formation mechanism. This study was also successful in keeping the collagen content low (25%) that may minimize the potential adverse effects of collagen degradation *in vivo*. We believe that this enhanced differentiation and

mineralization observed in the case of our H4 composite can be attributed to its higher matrix stiffness, which significantly affects the microstructural cues presented to the stem cells and elevates the degree of their osteogenic response. For example, Tan et al. reported a synergistic effect of matrix stiffness and BMP-2 on MSCs, supporting the contention that extrinsic factors affect the fate of these cells [26]. Banks et al. showed that the stiffer collagen-glycosaminoglycan substrates direct osteogenic lineage commitment of adipose stem cells regardless of presence or absence of growth factors [31]. The data in our study thus supported the hypothesis that a stiffer scaffold will mimic a similar extracellular microenvironment of native bone cells and signal the cells to proliferate, differentiate, and mineralize to a greater extent. Future studies are needed to find the optimal ELP and collagen composition to further improve the mechanical properties of these composites for a successful use in GBR. We feel that a longer duration study may be needed in order to achieve better differentiation and maturation for a significant formation of the bone-like tissue. These results will also need further validation *in vivo*.

5. CONCLUSION

The incorporation of ELP into the collagen matrix resulted in the improvement of the mechanical properties of the composites. Our results show that the composite containing higher concentrations of ELP and collagen (18:6 mg/mL) to be a suitable scaffold for the long-term, 3-dimensional culture and the subsequent osteogenic differentiation of hASCs resulting in superior mineralization. This study holds a great promise for developing ELP-collagen composite scaffolds in guided bone regeneration with further studies focusing on the evaluation of their efficacy *in vivo*.

Acknowledgments

Sponsored by the National Institute of Dental and Craniofacial Research of the National Institutes of Health under Award Number R03DE024257. The content is solely the responsibility of the authors and does not necessarily represent the official views of the National Institutes of Health. PCB participated in the Undergraduate and Professional Student Training in Advanced Research Techniques (UPSTART) Program. This work made use of instruments in the Department of Biomedical Materials Science User Facility. We thank Dr. Peter Arnold for the procurement of the donated whole adipose tissue.

REFERENCES

1. Fujihara K, Kotaki M, Ramakrishna S. Guided bone regeneration membrane made of polycaprolactone/calcium carbonate composite nano-fibers. Biomaterials. 2005; 26:4139–4147. [PubMed: 15664641]
2. Cortellini P, Stalpers G, Mollo A, Tonetti MS. Periodontal regeneration versus extraction and prosthetic replacement of teeth severely compromised by attachment loss to the apex: 5-year results of an ongoing randomized clinical trial. J Clin Periodontol. 2011; 38:915–924. [PubMed: 21777268]
3. Bottino MC, Thomas V, Schmidt G, Vohra YK, Chu TM, Kowolik MJ, Janowski GM. Recent advances in the development of GTR/GBR membranes for periodontal regeneration -a materials perspective. Dent Mater. 2012; 28:703–721. [PubMed: 22592164]
4. Qi H, Aguiar DJ, Williams SM, La Pean A, Pan W, Verfaillie CM. Identification of genes responsible for osteoblast differentiation from human mesodermal progenitor cells. Proc Natl Acad Sci U S A. 2003; 100:3305–3310. [PubMed: 12631704]

5. Strem BM, Hicok KC, Zhu M, Wulur I, Alfonso Z, Schreiber RE, Fraser JK, Hedrick MH. Multipotential differentiation of adipose tissue-derived stem cells. Keio J Med. 2005; 54:132–141. [PubMed: 16237275]
6. Zuk PA, Zhu M, Ashjian P, De Ugarte DA, Huang JI, Mizuno H, Alfonso ZC, Fraser JK, Benhaim P, Hedrick MH. Human adipose tissue is a source of multipotent stem cells. Mol Biol Cell. 2002; 13:4279–4295. [PubMed: 12475952]
7. Lendeckel S, Jodicke A, Christophis P, Heidinger K, Wolff J, Fraser JK, Hedrick MH, Berthold L, Howaldt HP. Autologous stem cells (adipose) and fibrin glue used to treat widespread traumatic calvarial defects: case report. J Craniomaxillofac Surg. 2004; 32:370–373. [PubMed: 15555520]
8. Mesimaki K, Lindroos B, Tornwall J, Mauno J, Lindqvist C, Kontio R, Miettinen S, Suuronen R. Novel maxillary reconstruction with ectopic bone formation by GMP adipose stem cells. Int J Oral Maxillofac Surg. 2009; 38:201–209. [PubMed: 19168327]
9. Milella E, Ramires PA, Brescia E, La Sala G, Di Paola L, Bruno V. Physicochemical, mechanical, and biological properties of commercial membranes for GTR. J Biomed Mater Res. 2001; 58:427–435. [PubMed: 11410902]
10. Kikuchi M, Koyama Y, Yamada T, Imamura Y, Okada T, Shirahama N, Akita K, Takakuda K, Tanaka J. Development of guided bone regeneration membrane composed of beta-tricalcium phosphate and poly (L-lactide-co-glycolide-co-epsilon-caprolactone) composites. Biomaterials. 2004; 25:5979–5986. [PubMed: 15183612]
11. Felipe ME, Andrade PF, Grisi MF, Souza SL, Taba M, Palioto DB, Novaes AB. Comparison of two surgical procedures for use of the acellular dermal matrix graft in the treatment of gingival recessions: a randomized controlled clinical study. J Periodontol. 2007; 78:1209–1217. [PubMed: 17608575]
12. Santos A, Goumenos G, Pascual A. Management of gingival recession by the use of an acellular dermal graft material: a 12-case series. J Periodontol. 2005; 76:1982–1990. [PubMed: 16274319]
13. Behring J, Junker R, Walboomers XF, Chessnut B, Jansen JA. Toward guided tissue and bone regeneration: morphology, attachment, proliferation, and migration of cells cultured on collagen barrier membranes A systematic review. Odontology. 2008; 96:1–11. [PubMed: 18661198]
14. Kyle S, Aggeli A, Ingham E, McPherson MJ. Production of self-assembling biomaterials for tissue enginering. Trends Biotech. 2009; 27:423–433.
15. Glowacki J, Mizuno S. Collagen scaffolds for tissue engineering. Biopolymers. 2008; 89:338–344. [PubMed: 17941007]
16. Speer DP, Chvapil M, Eskelson CD, Ulreich J. Biological effects of residual glutaraldehyde in glutaraldehyde-tanned collagen biomaterials. J Biomed Mater Res. 1980; 14:753–764. [PubMed: 6820019]
17. Wang L, Stegemann JP. Glyoxal crosslinking of cell-seeded chitosan/collagen hydrogels for bone regeneration. Acta Biomater. 2011; 7:2410–2417. [PubMed: 21345389]
18. Amruthwar SS, Janorkar AV. Preparation and characterization of elastin-like polypeptide scaffolds for local delivery of antibiotics and proteins. J Mater Sci Mater Med. 2012; 23:2903–2912. [PubMed: 22926272]
19. Annabi N, Mithieux SM, Boughton EA, Ruys AJ, Weiss AS, Dehghani F. Synthesis of highly porous crosslinked elastin hydrogels and their interaction with fibroblasts in vitro. Biomaterials. 2009; 30:4550–4557. [PubMed: 19500832]
20. MacEwan SR, Chilkoti A. Elastin-like polypeptides: biomedical applications of tunable biopolymers. Biopolymers. 2010; 94:60–77. [PubMed: 20091871]
21. Meyer DE, Chilkoti A. Purification of recombinant proteins by fusion with thermally-responsive polypeptides. Nat Biotechnol. 1999; 17:1112–1115. [PubMed: 10545920]
22. Bottino MC, Thomas V, Janowski GM. A novel spatially designed and functionally graded electrospun membrane for periodontal regeneration. Acta Biomater. 2011; 7:216–224. [PubMed: 20801241]
23. Urry DW. Physical chemistry of biological free energy transduction as demonstrated by elastin protein-based polymers. J Phys. Chem. 1997; 101:11007–11028.

24. Amruthwar SS, Puckett AD, Janorkar AV. Preparation and characterization of novel elastin-like polypeptide-collagen composites. J Biomed Mater Res A. 2013; 101:2383–2391. [PubMed: 23427027]
25. Amruthwar SS, Janorkar AV. In vitro evaluation of elastin-like polypeptide-collagen composite. Dent Mater. 2013; 29:211–220. [PubMed: 23127995]
26. Tan S, Fang JY, Yang Z, Nimni ME, Han B. The synergetic effect of hydrogel stiffness and growth factor on osteogenic differentiation. Biomaterials. 2014; 35:5294–5306. [PubMed: 24703716]
27. Parekh SH, Chatterjee K, Lin-Gibson S, Moore NM, Cicerone MT, Young MF, Simon CG Jr. Modulus-driven differentiation of marrow stromal cells in 3D scaffolds that is independent of myosin-based cytoskeletal tension. Biomaterials. 2011; 32:2256–2264. [PubMed: 21176956]
28. Huebsch N, Arany PR, Mao AS, Shvartsman D, Ali OA, Bencherif SA, Rivera-Feliciano J, Mooney DJ. Harnessing traction-mediated manipulation of the cell/matrix interface to control stem-cell fate. Nature Materials. 2010; 9:518–526. [PubMed: 20418863]
29. Wheeler TS, Sbravati ND, Janorkar AV. Mechanical & cell culture properties of elastin-like polypeptide, collagen, bioglass, and carbon nanosphere composites. Annals Biomed Eng. 2013; 41:2042–2055.
30. Salasznyk RM, Williams WA, Boskey A, Batorsky A, Plopper GE. Adhesion to vitronectin and collagen I promotes osteogenic differentiation of human mesenchymal stem cells. J Biomed Biotechnol. 2004; 2004:24–34. [PubMed: 15123885]
31. Banks JM, Mozdzen LC, Harley BA, Bailey RC. The combined effects of matrix stiffness and growth factor immobilization on the bioactivity and differentiation capabilities of adipose-derived stem cells. Biomaterials. 2014; 35:8951–8959. [PubMed: 25085859]
32. Niu LN, Jiao K, Qi YP, Nikonov S, Yiu CK, Arola DD, Gong SQ, El-Marakby A, Carrilho MR, Hamrick MW, Hargreaves KM, Diogenes A, Chen JH, Pashley DH, Tay FR. Intrafibrillar silicification of collagen scaffolds for sustained release of stem cell homing chemokine in hard tissue regeneration. FASEB J. 2012; 26:4517–4529. [PubMed: 22859369]
33. Brougham CM, Levingstone TJ, Jockenhoevel S, Flanagan TC, O'Brien FJ. Incorporation of fibrin into a collagen-glycosaminoglycan matrix results in a scaffold with improved mechanical properties and enhanced capacity to resist cell-mediated contraction. Acta Biomater. 2015; 26:205–214. [PubMed: 26297884]
34. Kuo YC, Yeh CF. Effect of surface-modified collagen on the adhesion, biocompatibility and differentiation of bone marrow stromal cells in poly(lactide-co-glycolide)/chitosan scaffolds. Colloids Surf B Biointerfaces. 2011; 82:624–631. [PubMed: 21074381]
35. Engler AJ, Sen S, Sweeney HL, Discher DE. Matrix elasticity directs stem cell lineage specification. Cell. 2006; 126:677–689. [PubMed: 16923388]
36. Killion JA, Geever LM, Devine DM, Kennedy JE, Higginbotham CL. Mechanical properties and thermal behavior of PEGDMA hydrogels for potential bone regeneration application. J Mech Behav Biomed Mater. 2011; 4:1219–1227. [PubMed: 21783130]
37. Zaborowska M, Bodin A, Backdahl H, Popp J, Goldstein A, Gatenholm P. Microporous bacterial cellulose as a potential scaffold for bone regeneration. Acta Biomater. 2010; 6:2540–2547. [PubMed: 20060935]
38. McCullen SD, Zhu Y, Bernacki SH, Narayan RJ, Pourdeyhimi B, Gorga RE, Loboa EG. Electrospun composite poly(L-lactic acid)/tricalcium phosphate scaffolds induce proliferation and osteogenic differentiation of human adipose-derived stem cells. Biomed Mater. 2009; 4:035002. [PubMed: 19390143]
39. Kang SW, Kim JS, Park KS, Cha BH, Shim JH, Kim JY, Cho DW, Rhie JW, Lee SH. Surface modification with fibrin/hyaluronic acid hydrogel on solid-free form-based scaffolds followed by BMP-2 loading to enhance bone regeneration. Bone. 2011; 48:298–306. [PubMed: 20870047]
40. Lu Z, Roohani-Esfahani SI, Wang G, Zreiqat H. Bone biomimetic microenvironment induces osteogenic differentiation of adipose tissue-derived mesenchymal stem cells. Nanomedicine. 2012; 8:507–515. [PubMed: 21839050]
41. Cooper, GM. The Cell: A Molecular Approach. 2nd. Sunderland (MA): Sinauer Associates; 2000. Cell Proliferation in Development and Differentiation. Available from: http://www.ncbi.nlm.nih.gov/books/NBK9906/

42. Zou L, Zou X, Chen L, Li H, Mygind T, Kassem M, Bunger C. Multilineage differentiation of porcine bone marrow stromal cells associated with specific gene expression pattern. J Orthop Res. 2008; 26:56–64. [PubMed: 17676606]
43. Serigano K, Sakai D, Hiyama A, Tamura F, Tanaka M, Mochida J. Effect of cell number on mesenchymal stem cell transplantation in a canine disc degeneration model. J Orthop Res. 2010; 28:1267–1275. [PubMed: 20839317]
44. Stucki U, Schmid J, Hammerle CF, Lang NP. Temporal local appearance of alkaline phosphatase activity in early stages of guided bone regeneration A descriptive histochemical study in humans. Clin Oral Implants Res. 2001; 12:121–127. [PubMed: 11251661]
45. Gerstenfeld LC, Chipman SD, Glowacki J, Lian JB. Expression of differentiated function by mineralizing cultures of chicken osteoblasts. Dev Biol. 1987; 122:49–60. [PubMed: 3496252]
46. Gandavarapu NR, Alge DL, Anseth KS. Osteogenic differentiation of human mesenchymal stem cells on alpha5 integrin binding peptide hydrogels is dependent on substrate elasticity. Biomater Sci. 2014; 2:352–361. [PubMed: 24660057]
47. Padovano JD, Ramachandran A, Bahmanyar S, Ravindran S, George A. Bone-specific overexpression of DMP1 influences osteogenic gene expression during endochondral and intramembranous ossification. Connect Tissue Res. 2014; (55 Suppl 1):121–124. [PubMed: 25158195]
48. Seibel MJ. Biochemical markers of bone turnover: part I: biochemistry and variability. Clin Biochem Rev. 2005; 26:97–122. [PubMed: 16648882]
49. Thein-Han W, Xu HH. Collagen-calcium phosphate cement scaffolds seeded with umbilical cord stem cells for bone tissue engineering. Tissue Eng Part A. 2011; 17:2943–2954. [PubMed: 21851269]
50. Heino J. The collagen receptor integrins have distinct ligand recognition and signaling functions. Matrix Biol. 2000; 19:319–323. [PubMed: 10963992]
51. Palecek SP, Loftus JC, Ginsberg MH, Lauffenburger DA, Horwitz AF. Integrin-ligand binding properties govern cell migration speed through cell-substratum adhesiveness. Nature. 1997; 385:537–540. [PubMed: 9020360]
52. Rezania A, Healy KE. Integrin subunits responsible for adhesion of human osteoblast-like cells to biomimetic peptide surfaces. J Orthop Res. 1999; 17:615–623. [PubMed: 10459771]
53. Tibbitt MW, Anseth KS. Hydrogels as extracellular matrix mimics for 3D cell culture. Biotechnol Bioeng. 2009; 103:655–663. [PubMed: 19472329]

Highlights

- Improved composite mechanical properties with higher ELP and collagen content
- Promoted proliferation of hASCs on ELP-collagen scaffolds
- Increased osteogenic differentiation with higher ELP and collagen content
- A promising composite scaffold for GBR application

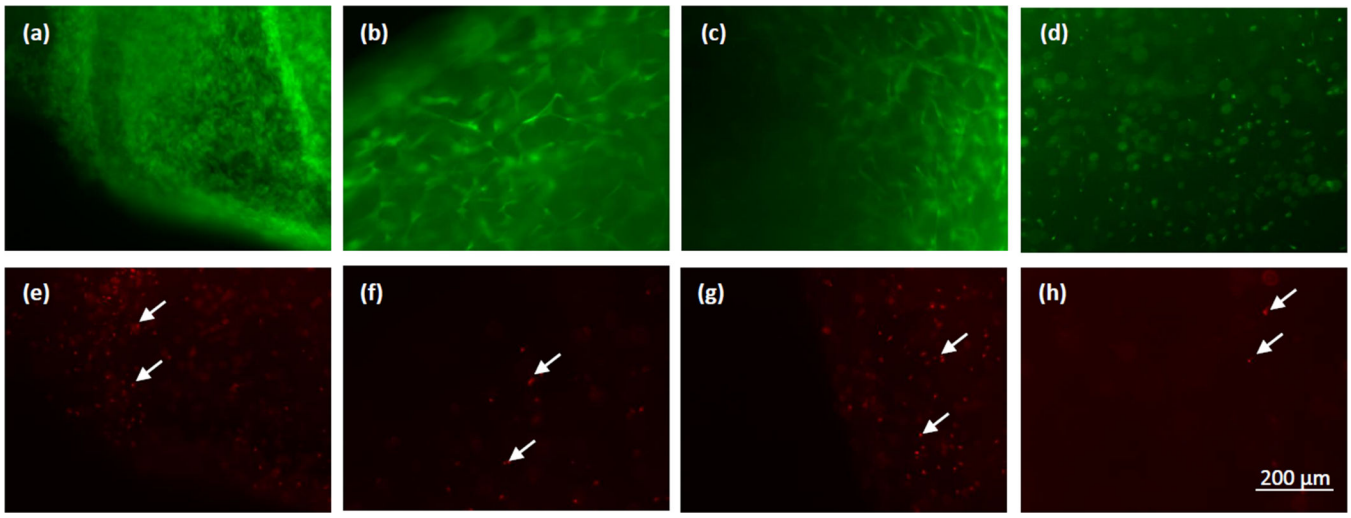

Figure 1.

Live/Dead images on day 22 with hASCs cultured within (a, e) H1 (b, f) H2 (c, g) H3 and (d, h) H4 composites showing live cells (top) and dead cells (bottom, shown by white arrows). Scale bar = 200 μm.

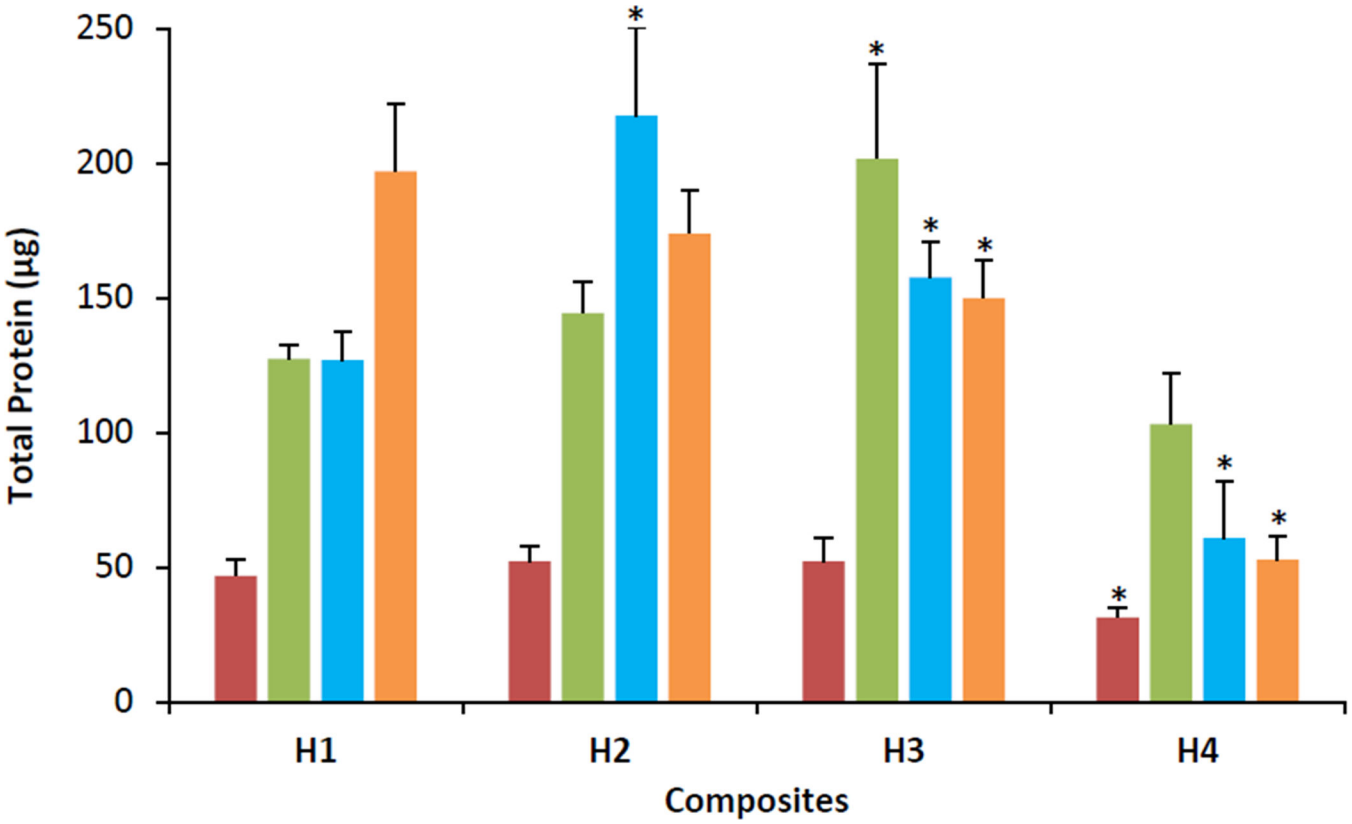

Figure 2.

Total protein content of hASCs cultured within H1, H2, H3 and H4 composites. Red bars = day 1; green bars = day 8; blue bars = day 15, orange bars = day 22. Error bars represent 95% confidence intervals. *$p \leq 0.05$ against H1 on the same day.

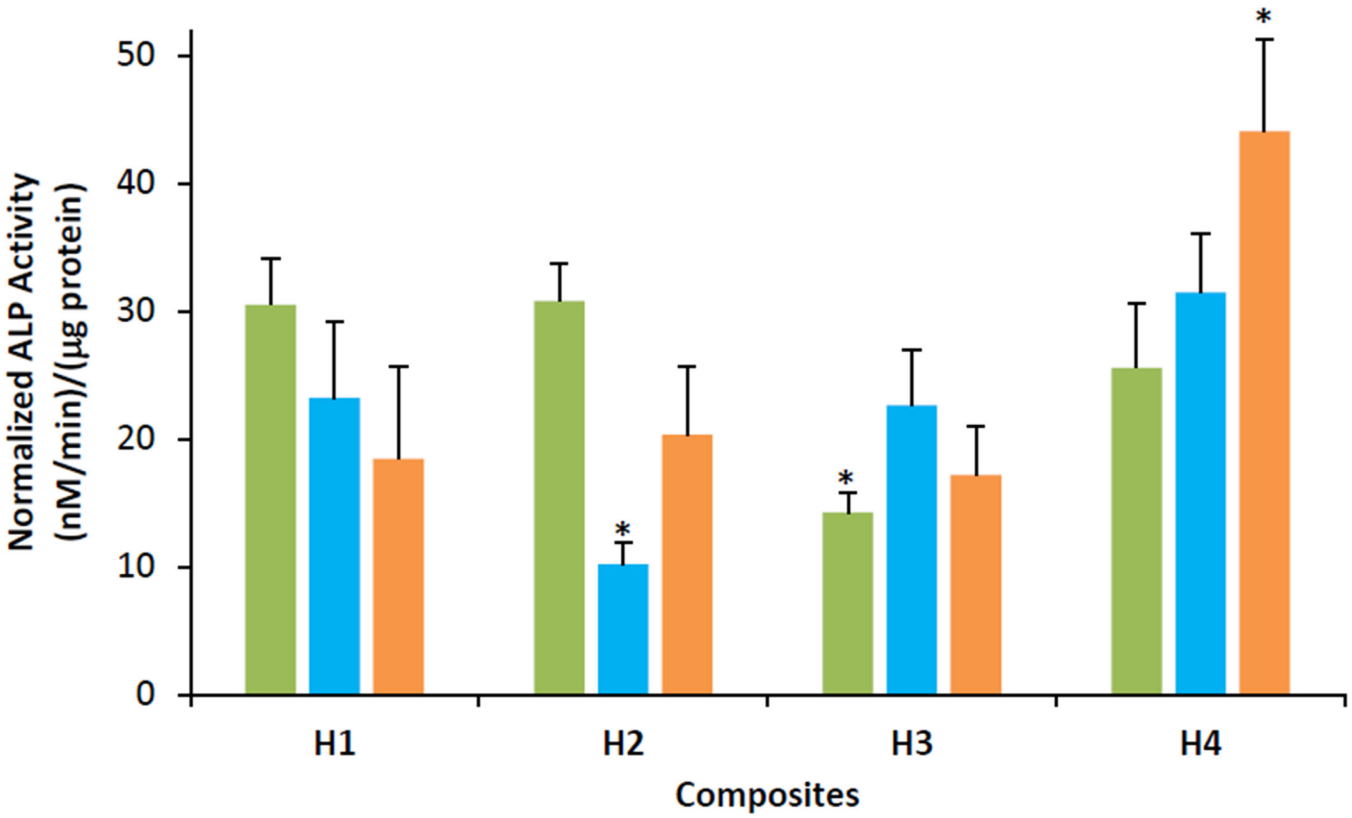

Figure 3.

ALP activity normalized to total protein of hASCs cultured within H1, H2, H3 and H4 composites. Green bars = day 8; blue bars = day 15, orange bars = day 22. Error bars represent 95% confidence intervals. *$p \leq 0.05$ against H1 on the same day.

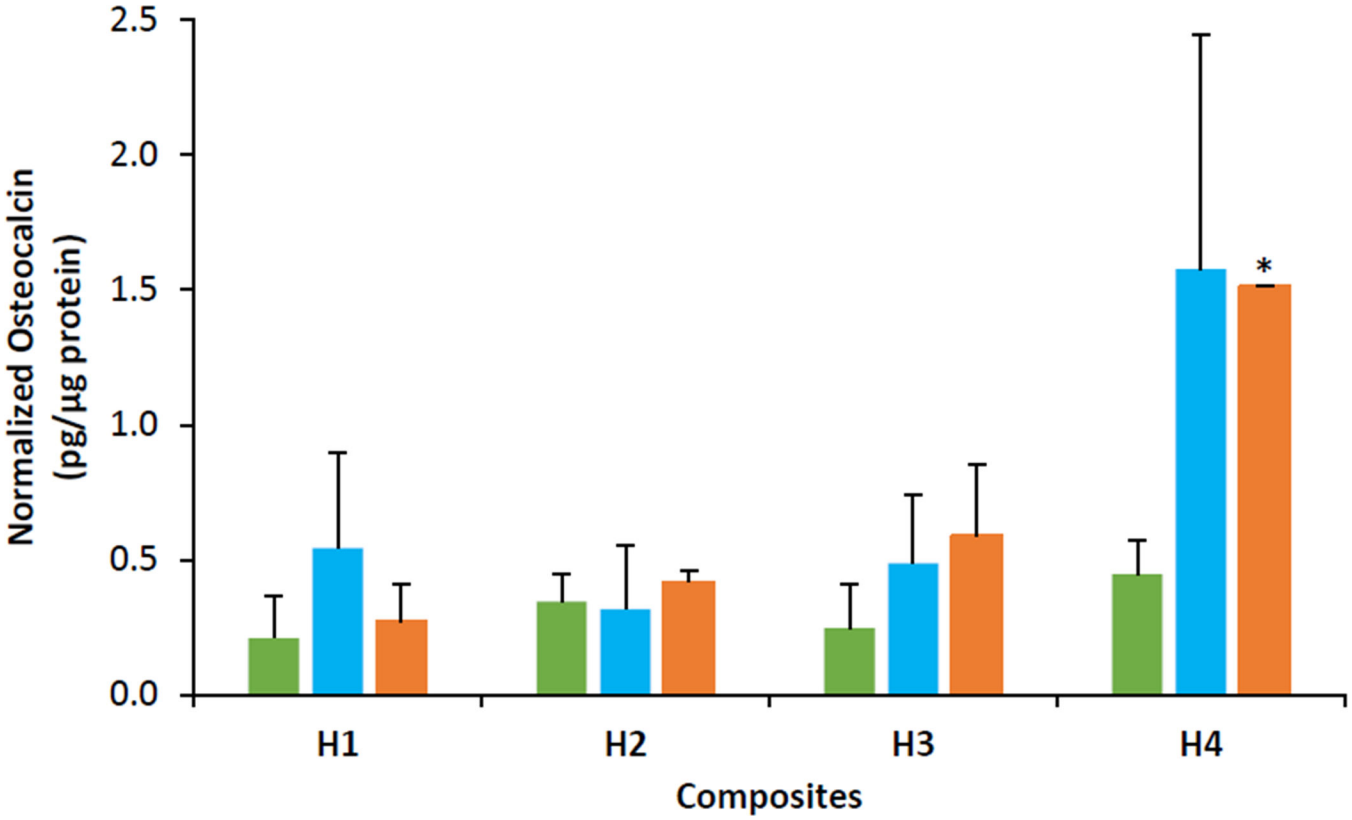

Figure 4.

Osteocalcin content normalized to total protein of hASCs cultured within H1, H2, H3 and H4 composites. Green bars = day 8; blue bars = day 15, orange bars = day 22. Error bars represent 95% confidence intervals. *$p \leq 0.05$ against H1 on the same day.

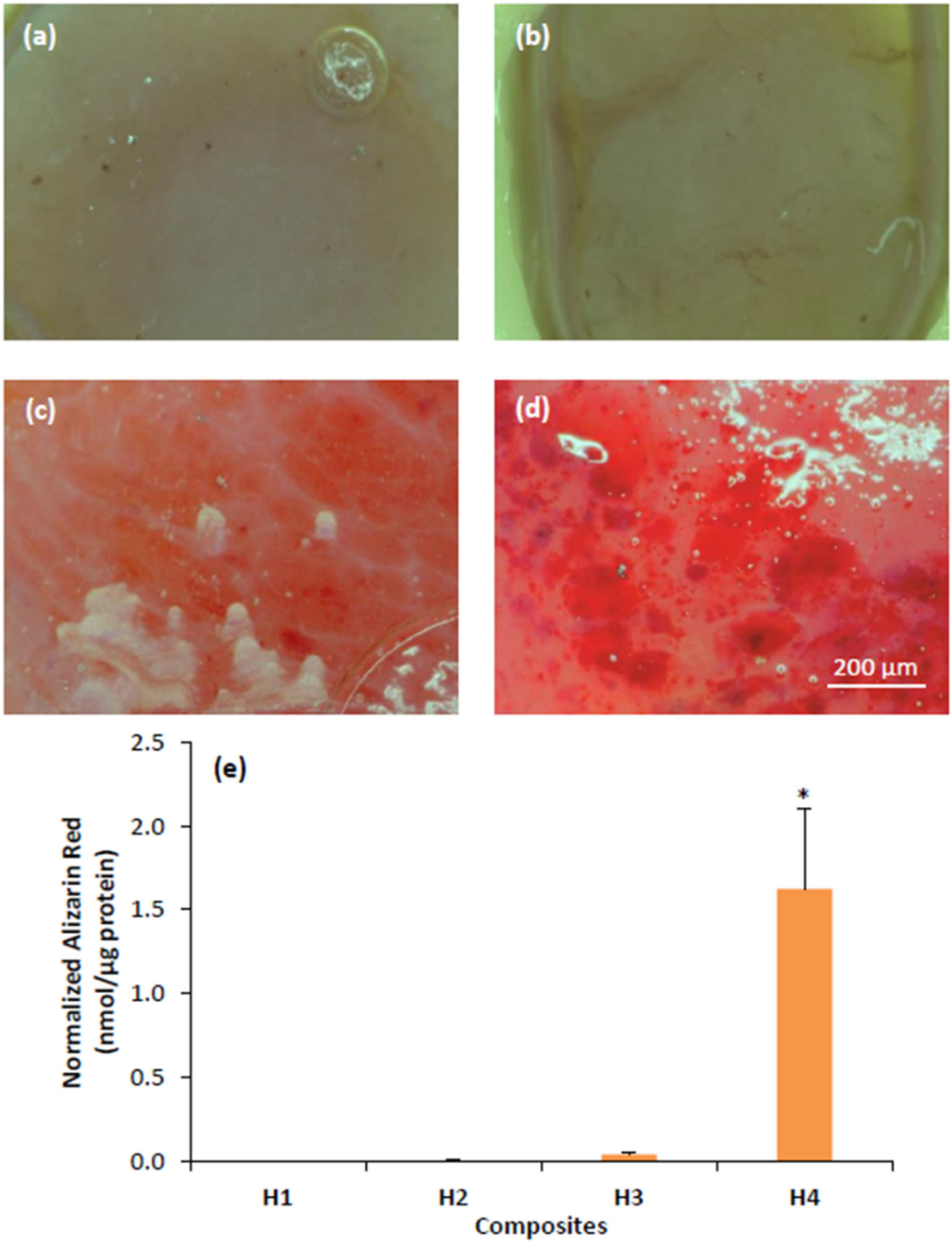

Figure 5.

Alizarin red staining of hASCs cultured within (a) H1, (b) H2, (c) H3 and (d) H4 composites on day 22. Scale bar = 200 µm. (e) Quantification of Alizarin red staining within the various composites normalized to total protein of hASCs. Error bars represent 95% confidence intervals. *$p \leq 0.05$ against H1 on the same day.

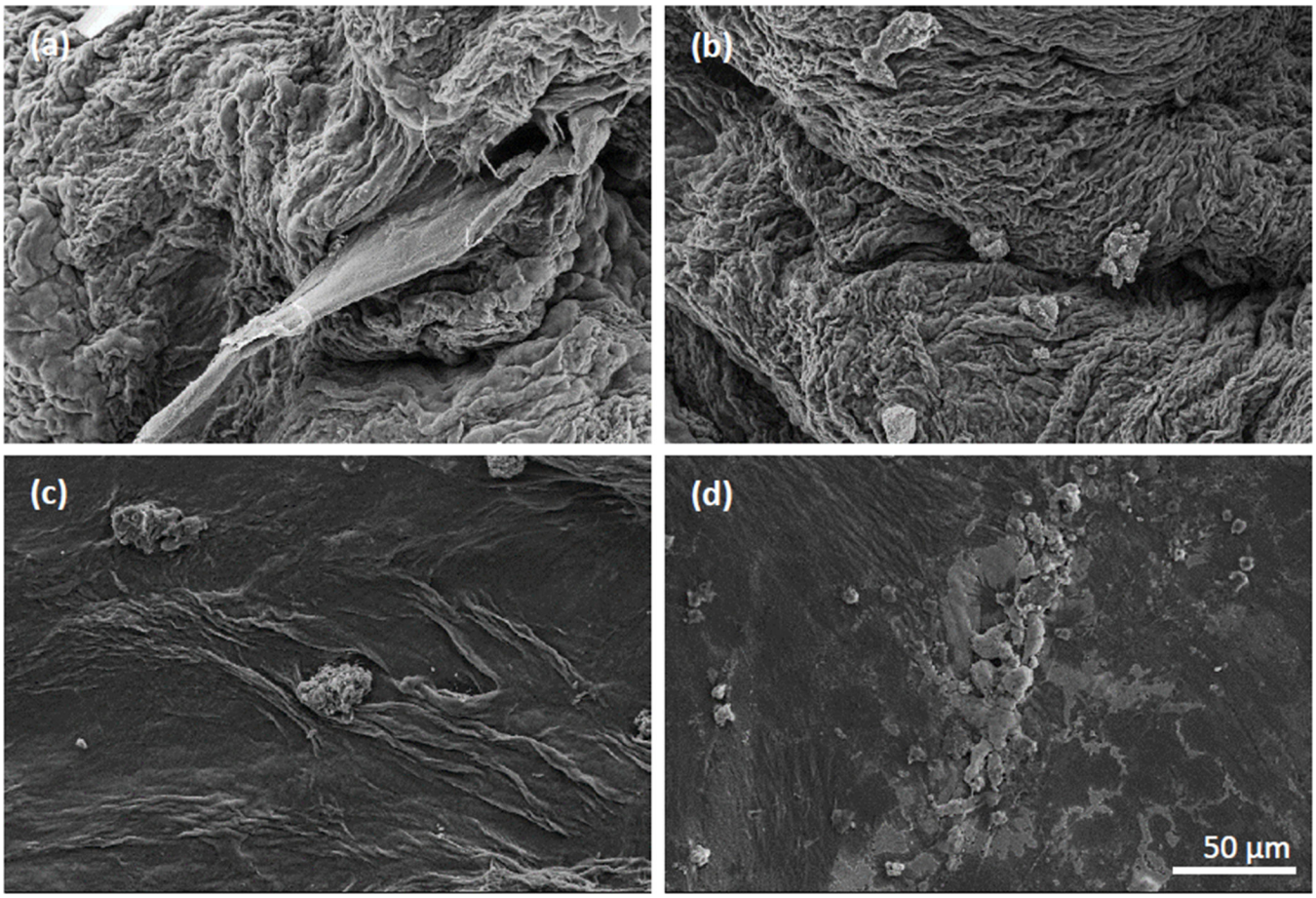

Figure 6.
SEM micrographs of dehydrated scaffolds. (a) H1, (b) H2, (c) H3, (d) H4. Scale bar = 50 µm.

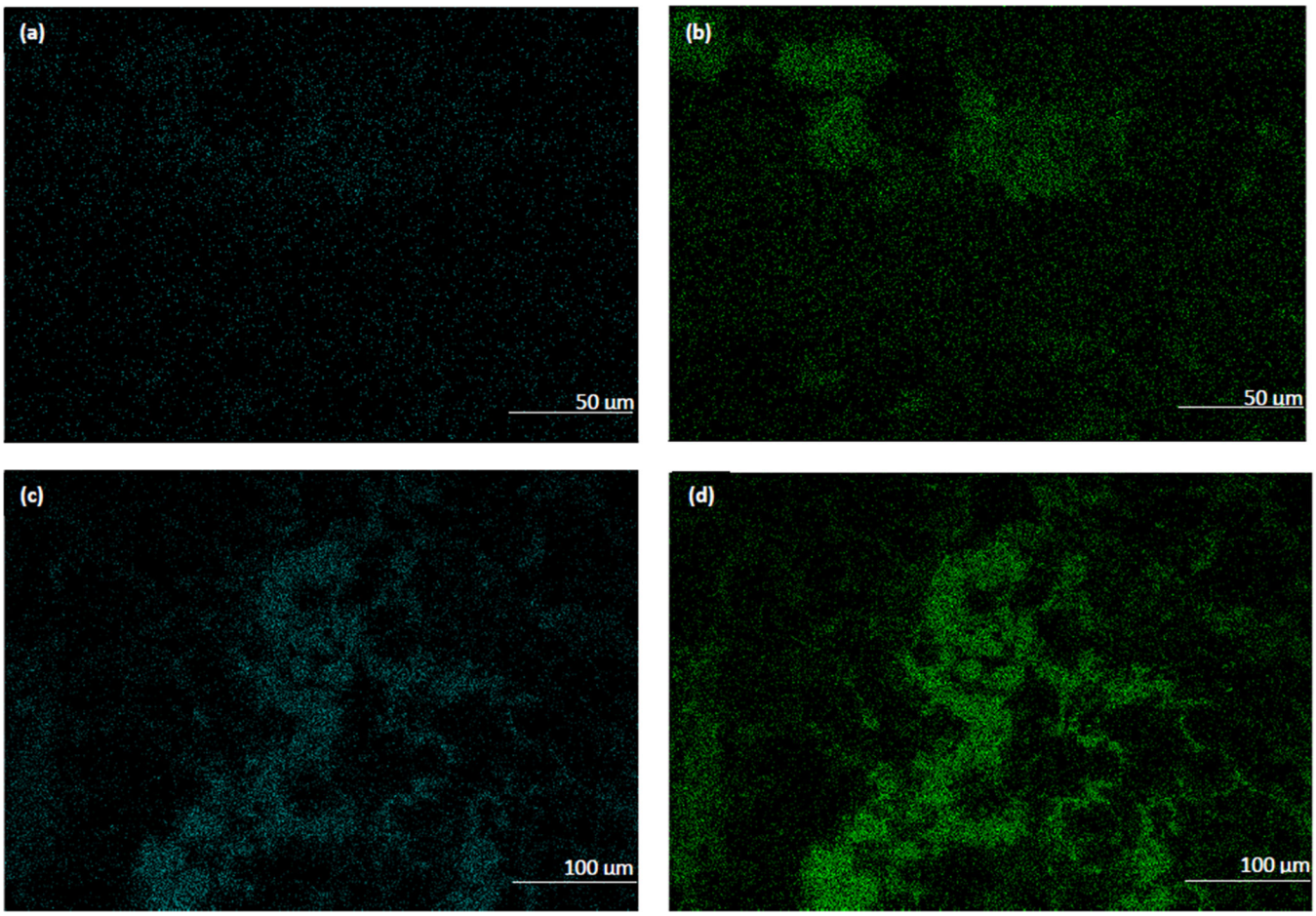

Figure 7.
Energy dispersive spectroscopy images showing deposition of (a, c) calcium and (b, d) phosphorous ions in (a, b) H3 and (c, d) H4 composites.

Table 1

Composition of scaffolds based on ELP and collagen content

Composite	ELP (mg/mL)	Collagen (mg/mL)	ELP-collagen ratio
H1	0	2	0
H2	6	2	3:1
H3	0	6	0
H4	18	6	3:1

Table 2

Mechanical properties of hydrated composites on day 8

Composite	Tensile Strength (kPa)	Elastic Modulus (kPa)	Toughness (kPa)
H1	12.7 ± 5.0	22.0 ± 11.2	0.16 ± 0.03
H2	13.7 ± 5.3	28.6 ± 9.7	0.17 ± 0.05
H3	14.6 ± 4.4	27.8 ± 8.4	0.27 ± 0.04 *
H4	20.2 ± 11.3	61. 8 ± 22.7 *	0.20 ± 0.04

* $p \leq 0.05$ against H1 on day 8